

Semi-parametric Models for Accelerated Destructive Degradation Test Data Analysis

Yimeng Xie¹, Caleb B. King¹, Yili Hong¹, and Qingyu Yang²

¹Department of Statistics, Virginia Tech, Blacksburg, VA 24061

²Department of Industrial and Systems Engineering, Wayne State University, Detroit, MI 48202

Abstract

Accelerated destructive degradation tests (ADDT) are widely used in industry to evaluate materials' long term properties. Even though there has been tremendous statistical research in nonparametric methods, the current industrial practice is still to use application-specific parametric models to describe ADDT data. The challenge of using a nonparametric approach comes from the need to retain the physical meaning of degradation mechanisms and also perform extrapolation for predictions at the use condition. Motivated by this challenge, we propose a semi-parametric model to describe ADDT data. We use monotonic B-splines to model the degradation path, which not only provides flexible models with few assumptions, but also retains the physical meaning of degradation mechanisms (e.g., the degradation path is monotonically decreasing). Parametric models, such as the Arrhenius model, are used for modeling the relationship between the degradation and accelerating variable, allowing for extrapolation to the use conditions. We develop an efficient procedure to estimate model parameters. We also use simulation to validate the developed procedures and demonstrate the robustness of the semi-parametric model under model misspecification. Finally, the proposed method is illustrated by multiple industrial applications.

Key Words: Acceleration model; ADDT; Arrhenius model; Degradation model; Long-term property evaluation; Polymeric materials.

1 Introduction

1.1 Motivation

It is important for manufacturers to understand the lifetime of their products in order to ensure accurate marketing and determine areas for improvement. While lifetime testing is the most common approach, for many materials it is more informative to observe the degradation of some performance characteristic, such as the tensile strength of an adhesive bond, over time. The lifetime is determined by a “soft failure” when the characteristic drops below a predetermined level. This form of testing is known as degradation testing.

Several varieties of degradation testing have been developed to accommodate unique circumstances. Due to the long service life of many new materials, degradation testing under normal use conditions is often not feasible. By exposing the material to a more harsh environment, such as higher levels of temperature or humidity compared to the use conditions, degradation data can be collected more efficiently. Thus, an accelerating variable is often used in degradation tests. In some applications, measurements of the degradation level are destructive. That is, the units being tested are destroyed or the physical characteristics changed in a significant manner. An example could be determining the strength of a material by measuring the force needed to break it. This form of testing, combined with an accelerating variable, is referred to as accelerated destructive degradation testing (ADDT). Because of the nature of the testing, ADDT must be analyzed differently from other common forms of degradation testing, such as repeated-measures degradation testing (RMDT), in which multiple measurements can be taken from the same unit.

Current procedures for analyzing ADDT data involve an assumed parametric model for the degradation path over time and a parametric form for the accelerating-variable effect. The predominance of parametric models is mainly due to the need for extrapolation in two aspects; extrapolation in time and extrapolation to the use conditions. For example, an ADDT may cover only 100-70% of the original material’s strength and be performed at an elevated temperature range (60–80°C), but interest lies at strengths 50-70% of the original at a temperature of 30°C. These parametric models tend to be material-specific and at present there seems to be no general model that can be applied to a wide variety of materials.

Even though there has been tremendous statistical research in nonparametric methods, the current industrial practice is still to use application-specific parametric models to describe ADDT data. Motivated by multiple industrial applications, we aim to bridge this gap between the statistical research and current industrial practice. Instead of a case-by-case parametric modeling approach, we propose a general and flexible semi-parametric model to

describe ADDT data. The challenge of using a nonparametric approach comes from the need to retain the physical meaning of degradation mechanisms and performing extrapolations for predictions at the use condition. To overcome those challenges, the semi-parametric model consists of a nonparametric model for the degradation path and a parametric form for the accelerating-variable effect. In order to preserve the monotonic nature of many degradation paths, the nonparametric model portion will be constructed based on monotonic spline methods. For the parametric model portion, commonly used models, such as the Arrhenius relationship for temperature, will be used for extrapolation. Parameter estimation and inference procedures will also be developed.

1.2 Related Literature

The literature on accelerated degradation data modeling and analysis can be divided into two areas: RMDT and ADDT. In the pioneering work, Lu and Meeker (1993) used RMDT data to estimate failure-time distribution via the framework on mixed-effects models. Meeker, Escobar, and Lu (1998) introduced nonlinear mixed-effects models for RMDT data, which were derived from physical-failure mechanisms. Introductory level description of degradation models can be found in Gorjian et al. (2010), and Meeker, Hong, and Escobar (2011). Ye and Xie (2015) provided a comprehensive review of the state-of-art methods in modeling RMDT data.

In the area of ADDT data modeling and analysis, Nelson (1990, Chapter 11) used ADDT data from an insulation to estimate performance degradation. Escobar et al. (2003) provided a parametric model and method to analyze the ADDT data collected from an adhesive bond. Tsai et al. (2013) considered the problem of designing an ADDT with a nonlinear model motivated by a polymer dataset. Li and Doganaksoy (2014) used a parametric model to model ADDT data collected from a temperature accelerated test to study the degradation of seal strength. In all existing methods for analyzing ADDT data, the parametric method is the most popular.

Compared to parametric models of degradation data, spline functions tend to be more flexible and require less assumptions regarding the model formulation. Because the degradation path is often monotonic in nature, monotone splines are suitable for modeling degradation paths. Ramsay (1988) suggested using a basis of I-splines (integrated splines) for semi-parametric modeling. He and Shi (1998) considered the use of B-splines with L_1 optimization. Meyer (2008) extended the work in Ramsay (1988) by proposing cubic monotone splines. Leitenstorfer and Tutz (2007) considered the use of monotone B-splines in generalized additive models. For other applications of monotone B-splines, one can refer to

Kanungo, Gay, and Haralick (1995) and Fengler and Hin (2014). In addition, Eilers and Marx (1996) proposed a flexible class of P-splines. Bollaerts, Eilers, and Mechelen (2006), Hofner, Müller, and Hothorn (2011), and Hofner, Kneib, and Hothorn (2014) considered the estimation of monotonic effects with P-splines.

Related to RMDT models, Ye et al. (2014) considered semi-parametric estimation of Gamma processes. Hong et al. (2015), and Xu, Hong, and Jin (2015) used shape-restricted splines to model the effects of time-varying covariates on the degradation process. There is little literature, however, on the use of semi-parametric models in ADDT data modeling and analysis.

1.3 Overview

The rest of this paper is organized as follows. Section 2 introduces some general notation for ADDT data. It also presents in detail the construction of the semi-parametric model using monotonic B-splines. In Section 3, we present a procedure for estimating the unknown parameters as well as procedures for conducting inference on ADDT data based on this model. We conduct simulation studies in Section 4 to investigate the performance of the semi-parametric method with special consideration of model misspecification. In Section 5, we apply the model to data from several published datasets and provide comparisons with other well-known parametric models. Finally, Section 6 contains conclusions and areas for future research.

2 The Semi-parametric Model

2.1 General Setting

Let y_{ijk} be the degradation measurement for the k th sample at level i of the accelerating variable \mathcal{AF}_i and the j th observation time point t_{ij} , $i = 1, \dots, I$, $j = 1, \dots, J_i$, and $k = 1, \dots, n_{ij}$, where n_{ij} denotes the sample size at t_{ij} . Let $n = \sum_{i=1}^I \sum_{j=1}^{J_i} n_{ij}$ be the total number of observations. A general form of the degradation model is

$$y_{ijk} = \mathcal{D}(t_{ij}, x_i; \boldsymbol{\theta}) + \varepsilon_{ijk}, \quad (1)$$

where $x_i = h(\mathcal{AF}_i)$ is a function of the accelerating variable, $\boldsymbol{\theta}$ is a vector of unknown parameters in the degradation path, and ε_{ijk} is an error term that describes unit-to-unit variability. For the purposes of illustration, we will assume that the degradation path is monotone decreasing with time. The model can easily be generalized to paths that are

increasing with time. We will also be considering temperature as the accelerating factor as it is the most common form of acceleration encountered in ADDT. However, the model can easily incorporate other types of acceleration, such as voltage.

For temperature-accelerated processes, the Arrhenius model is often used to describe the relationship between degradation and temperature. This model uses a transformed temperature level given as

$$x_i = \frac{-11605}{\text{Temp}_i + 273.16}. \quad (2)$$

Here, Temp_i is in degrees Celsius, and 11605 is the reciprocal of the Boltzmann's constant (in units of eV). The value 273.16 in the denominator is used to convert to the Kelvin temperature scale.

2.2 The Scale Acceleration Model

We propose the following semi-parametric functional forms for the degradation model in (1).

$$\mathcal{D}(t_{ij}, x_i; \boldsymbol{\theta}) = g[\eta_i(t_{ij}; \beta); \boldsymbol{\gamma}], \quad (3)$$

$$\eta_i(t; \beta) = \frac{t}{\exp(\beta s_i)}, \quad s_i = x_{\max} - x_i, \quad (4)$$

$$\varepsilon_{ijk} \sim N(0, \sigma^2), \quad \text{and} \quad \text{Corr}(\varepsilon_{ijk}, \varepsilon_{ijk'}) = \rho, \quad k \neq k'. \quad (5)$$

Here, $g(\cdot)$ is a monotone decreasing function with unknown parameter vector $\boldsymbol{\gamma}$, β is an unknown parameter associated with the accelerating variable, and $\boldsymbol{\theta} = (\boldsymbol{\gamma}', \beta, \sigma, \rho)'$ is the vector containing all of the unknown parameters. The quantity $x_{\max} = -11605/[\max_i(\text{Temp}_i) + 273.16]$ is defined to be the transformed value of the highest level of the accelerating variable.

The model in (3) falls within the class of scale acceleration models. For a specific stress level i , $\mathcal{D}(t, x_i; \boldsymbol{\theta})$ is a decreasing function of time t , in which β controls the degradation rate through time-scale factor $\exp(\beta s_i)$ in (4). A smaller time-scale factor corresponds to a rapid decrease in degradation. When the acceleration level is at its highest, $s_{\max} = x_{\max} - x_{\max} = 0$. In this case, $\eta_i(t; \beta) = t$ implies that the degradation path no longer relies on β , and

$$\mathcal{D}(t, x_{\max}; \boldsymbol{\theta}) = g(t; \boldsymbol{\gamma}).$$

Thus, the function $g(\cdot)$ can be interpreted as the baseline degradation path for the scale acceleration model in (3). The distribution of error terms ε_{ijk} are specified in (5) with parameters σ and ρ . In particular, we consider a compound symmetric correlation structure for measurements taken on the same temperature and time point. Measurements at different temperatures and times are assumed to be independent.

Let y_M be the lowest degradation level present in the observed data. Then the scale-acceleration model and the monotonicity of $g(\cdot)$ will allow one to extrapolate the degradation level to y_M for any given acceleration level. Let \mathcal{D}_f be the failure threshold. Then, if $y_M < \mathcal{D}_f$, one can use the semi-parametric model to obtain failure information at the use conditions through this extrapolation. This is particularly useful since, in general, measurements may be available below \mathcal{D}_f for only some of the highest levels of the accelerating variable. In fact, some industrial standards require that tests be run until the degradation level drops below \mathcal{D}_f for several acceleration levels. However, extrapolation beyond y_M is not possible due to the nonparametric construction of the $g(\cdot)$, which is the tradeoff for this kind of model flexibility.

2.3 Nonparametric Form for Baseline Degradation Path

We use nonparametric methods to estimate the baseline degradation path $g(\cdot)$. Specifically, we use monotonic B-splines to model the baseline degradation path. This not only provides flexible models, but also retains the physical meaning of degradation mechanisms (e.g., the degradation path is monotonically decreasing).

Consider a set of interior knots $d_1 \leq \dots \leq d_N$, and two boundary points d_0 and d_{N+1} . The entire set of ordered knots are

$$d_{-q} = \dots = d_0 \leq d_1 \leq \dots \leq d_N \leq d_{N+1} = \dots = d_{N+q+1},$$

where the lower and upper boundary points are appended q times and q is the polynomial degree. For notational simplicity, we rewrite the subscripts in the ordered knot sequences as d_1, \dots, d_{N+2q+2} . The total number of basis functions is $p = N + q + 1$. The l th B-spline basis function of degree q evaluated at z can be recursively obtained in the following formulas:

$$B_{0,l}(z) = \mathbf{1}(d_l \leq z < d_{l+1}),$$

$$B_{q,l}(z) = \frac{z - d_l}{d_{l+q} - d_l} B_{q-1,l}(z) + \frac{d_{l+q+1} - z}{d_{l+q+1} - d_{l+1}} B_{q-1,l+1}(z),$$

where $l = 1, \dots, p$, and $\mathbf{1}(\cdot)$ is an indicator function. The degradation model can then be expressed as

$$y_{ijk} = \sum_{l=1}^p \gamma_l B_{q,l}[\eta_i(t_{ij}; \beta)] + \varepsilon_{ijk}, \quad (6)$$

where γ_l 's are the coefficients.

To ensure the degradation path is monotone decreasing, we require the first derivative of $\mathcal{D}(\tau_{ij}, x_i; \boldsymbol{\theta})$ be negative. For B-spline basis functions, De Boor (2001) proved that the

derivative of $\mathcal{D}(t, x_i; \boldsymbol{\theta})$ with respect to $\eta_i(t; \beta)$ is

$$\frac{d\mathcal{D}(t, x_i; \boldsymbol{\theta})}{d\eta_i(t; \beta)} = \sum_{l=2}^p (q-1) \frac{(\gamma_l - \gamma_{l-1})}{d_{l+q+1} - d_l} B_{q-1,l}[\eta_i(t; \beta)].$$

As B-spline basis functions are nonnegative, it follows that $\gamma_l \leq \gamma_{l-1}$ for all $2 \leq l \leq p$ gives a sufficient condition for a monotone decreasing degradation path. However, except for basis functions with degree $q = 1, 2$, it is not a necessary condition. Fritsch and Carlson (1980) derived the necessary conditions for cubic splines ($q = 3$), though for higher order splines necessary conditions are as yet unclear.

3 Estimation and Inference

3.1 Parameter Estimation

Let $\mathbf{y}_{ij} = (y_{ij1}, \dots, y_{ijn_{ij}})'$, $\boldsymbol{\varepsilon}_{ij} = (\varepsilon_{ij1}, \dots, \varepsilon_{ijn_{ij}})'$, $\mathbf{y} = (y'_{11}, \dots, y'_{1J_1}, \dots, y'_{I1}, \dots, y'_{IJ_I})'$, $\boldsymbol{\varepsilon} = (\varepsilon'_{11}, \dots, \varepsilon'_{1J_1}, \dots, \varepsilon'_{I1}, \dots, \varepsilon'_{IJ_I})'$ and $\boldsymbol{\gamma} = (\gamma_1, \dots, \gamma_p)'$. The degradation model in (6) can be written as

$$\mathbf{y} = \mathbf{X}_\beta \boldsymbol{\gamma} + \boldsymbol{\varepsilon}, \quad (7)$$

where

$$\mathbf{X}_\beta = \begin{bmatrix} B_{q,1}[\eta_1(t_{11}; \beta)] & \cdots & B_{q,p}[\eta_1(t_{11}; \beta)] \\ B_{q,1}[\eta_1(t_{12}; \beta)] & \cdots & B_{q,p}[\eta_1(t_{12}; \beta)] \\ \vdots & \ddots & \vdots \\ B_{q,1}[\eta_I(t_{IJ_I}; \beta)] & \cdots & B_{q,p}[\eta_I(t_{IJ_I}; \beta)] \end{bmatrix},$$

and $\boldsymbol{\varepsilon} \sim N(\mathbf{0}, \boldsymbol{\Sigma})$. Here, $\boldsymbol{\Sigma} = \text{Diag}(\boldsymbol{\Sigma}_{11}, \dots, \boldsymbol{\Sigma}_{1J_1}, \dots, \boldsymbol{\Sigma}_{I1}, \dots, \boldsymbol{\Sigma}_{IJ_I})$ and $\boldsymbol{\Sigma}_{ij} = \sigma^2[(1 - \rho)I_{n_{ij}} + \rho J_{n_{ij}}]$, where $I_{n_{ij}}$ is an $n_{ij} \times n_{ij}$ identity matrix and $J_{n_{ij}}$ is an $n_{ij} \times n_{ij}$ matrix of 1's. We can also rewrite $\boldsymbol{\Sigma} = \sigma^2 \mathbf{R}$, where $\mathbf{R} = \text{Diag}(\mathbf{R}_{11}, \dots, \mathbf{R}_{1J_1}, \dots, \mathbf{R}_{I1}, \dots, \mathbf{R}_{IJ_I})$ and $\mathbf{R}_{ij} = (1 - \rho)I_{n_{ij}} + \rho J_{n_{ij}}$.

We use likelihood-based methods to estimate the unknown parameters $\boldsymbol{\theta} = (\boldsymbol{\gamma}', \beta, \sigma, \rho)'$. For now, we consider estimation of $\boldsymbol{\theta}$ with a given number of knots and knot locations. We will give a discussion on knot selection in Section 3.2. A particular challenge to the estimation comes from the constraints on $\boldsymbol{\gamma}$, namely that $\gamma_l \leq \gamma_{l-1}$, $2 \leq l \leq p$. We also note that, for a given β , \mathbf{X}_β is known, in which case (7) becomes a linear model with a correlated covariance structure. Thus, we proceed by first deriving estimates of $(\boldsymbol{\gamma}', \sigma, \rho)'$ given β and then use a profile likelihood approach to estimate β .

The estimates of $\boldsymbol{\gamma}$ and $(\sigma, \rho)'$ are obtained using an iterative procedure. In particular, at the m th iteration, given estimates $(\hat{\sigma}^{(m-1)}, \hat{\rho}^{(m-1)})'$, the value of $\hat{\boldsymbol{\gamma}}^{(m)}$ is obtained by

minimizing

$$Q(\boldsymbol{\gamma}) = (\mathbf{y} - \mathbf{X}_\beta \boldsymbol{\gamma})' \left(\widehat{\boldsymbol{\Sigma}}^{(m-1)} \right)^{-1} (\mathbf{y} - \mathbf{X}_\beta \boldsymbol{\gamma})$$

subject to $\gamma_l \leq \gamma_{l-1}, 2 \leq l \leq p.$

(8)

Equation (8) is a quadratic object function with linear constraints and so can be solved with quadratic programming techniques. Given $\widehat{\boldsymbol{\gamma}}^{(m)}$, one can then obtain $(\widehat{\sigma}^{(m)}, \widehat{\boldsymbol{\rho}}^{(m)})'$ using restricted maximum likelihood (REML) so long as $\widehat{\boldsymbol{\gamma}}^{(m)}$ does not take values on the boundary of the linear constraints. If the solution of equation (8) does take values on the boundary of the linear constraints, we can still consider approximate REML to obtain these estimates. Let $\widehat{\boldsymbol{\gamma}}_u^{(m)}$ represent all of the unique values in $\widehat{\boldsymbol{\gamma}}^{(m)}$ and p_u be the length of $\widehat{\boldsymbol{\gamma}}_u^{(m)}$. For each unique value $\widehat{\gamma}_{i,u}^{(m)}$, let $\mathbf{x}_{i,\beta u}$ be the sum of the corresponding columns in \mathbf{X}_β . Then we have $\mathbf{X}_\beta \widehat{\boldsymbol{\gamma}}^{(m)} = \mathbf{X}_{\beta u} \widehat{\boldsymbol{\gamma}}_u^{(m)}$, where $\mathbf{X}_{\beta u} = (\mathbf{x}_{1,\beta u}, \dots, \mathbf{x}_{p_u,\beta u})$. The approximate REML log-likelihood is then

$$\mathcal{L}_{\text{REML}}(\sigma, \boldsymbol{\rho} | \widehat{\boldsymbol{\gamma}}^{(m)}) = -\frac{1}{2} \left\{ \log |\boldsymbol{\Sigma}| + \log |\mathbf{X}'_{\beta u} \boldsymbol{\Sigma}^{-1} \mathbf{X}_{\beta u}| + (\mathbf{y} - \mathbf{X}_\beta \widehat{\boldsymbol{\gamma}}^{(m)})' \boldsymbol{\Sigma}^{-1} (\mathbf{y} - \mathbf{X}_\beta \widehat{\boldsymbol{\gamma}}^{(m)}) \right\}.$$
(9)

The covariance parameter estimates $(\widehat{\sigma}^{(m)}, \widehat{\boldsymbol{\rho}}^{(m)})'$ are those values that maximize equation (9). In particular, after some calculation it can be shown that $\widehat{\sigma}^{(m)}$ has the following closed-form expression

$$\widehat{\sigma}^{(m)} = \left[\frac{(\mathbf{y} - \mathbf{X}_\beta \widehat{\boldsymbol{\gamma}}^{(m)})' (\widehat{\mathbf{R}}^{(m-1)})^{-1} (\mathbf{y} - \mathbf{X}_\beta \widehat{\boldsymbol{\gamma}}^{(m)})}{n - p_u} \right]^{\frac{1}{2}}.$$

Thus, $\widehat{\boldsymbol{\rho}}^{(m)}$ can be obtained from a one dimensional optimization problem. That is,

$$\widehat{\boldsymbol{\rho}}^{(m)} = \underset{\boldsymbol{\rho}}{\text{argmax}} \left\{ -\log |(\widehat{\sigma}^{(m)})^2 \mathbf{R}| - \log |(\widehat{\sigma}^{(m)})^{-2} \mathbf{X}'_{\beta u} \mathbf{R}^{-1} \mathbf{X}_{\beta u}| \right. \\ \left. - (\widehat{\sigma}^{(m)})^{-2} (\mathbf{y} - \mathbf{X}_\beta \widehat{\boldsymbol{\gamma}}^{(m)})' \mathbf{R}^{-1} (\mathbf{y} - \mathbf{X}_\beta \widehat{\boldsymbol{\gamma}}^{(m)}) \right\}.$$

Upon convergence, the estimates of $(\widehat{\boldsymbol{\gamma}}', \widehat{\sigma}, \widehat{\boldsymbol{\rho}})'$ are obtained for a given β , denoted by $(\widehat{\boldsymbol{\gamma}}'_\beta, \widehat{\sigma}_\beta, \widehat{\boldsymbol{\rho}}_\beta)'$. The initial values $(\widehat{\sigma}^{(0)}, \widehat{\boldsymbol{\rho}}^{(0)})'$ can be easily obtained by fitting a non-constrained model.

The profile log-likelihood for β is given as

$$\mathcal{L}(\beta, \widehat{\boldsymbol{\gamma}}_\beta, \widehat{\sigma}_\beta, \widehat{\boldsymbol{\rho}}_\beta) = \log \left\{ \frac{1}{\sqrt{2\pi} |\widehat{\boldsymbol{\Sigma}}_\beta|^{1/2}} \exp \left[-\frac{(\mathbf{y} - \mathbf{X}_\beta \widehat{\boldsymbol{\gamma}}_\beta)' \widehat{\boldsymbol{\Sigma}}_\beta^{-1} (\mathbf{y} - \mathbf{X}_\beta \widehat{\boldsymbol{\gamma}}_\beta)}{2} \right] \right\}.$$

In practice, one can first estimate $(\boldsymbol{\gamma}', \sigma, \boldsymbol{\rho})'$ for a specified range of values of β , then compute $\mathcal{L}(\beta, \widehat{\boldsymbol{\gamma}}_\beta, \widehat{\sigma}_\beta, \widehat{\boldsymbol{\rho}}_\beta)$ as a function of β . The estimate $\widehat{\beta}$ is the value that maximizes this function. The final estimates are denoted by $\widehat{\boldsymbol{\theta}} = (\widehat{\boldsymbol{\gamma}}', \widehat{\beta}, \widehat{\sigma}, \widehat{\boldsymbol{\rho}})'$.

Once the model parameters have been estimated, other parameters related to reliability can then be estimated. For example, the mean time to failure (MTTF), denoted by m_f , is one of many ways to evaluate the reliability of a product/material. Based on the semi-parametric model, we can derive an estimate \hat{m}_f at a use condition x_f and failure threshold \mathcal{D}_f by solving

$$\sum_{l=1}^p \hat{\gamma}_l B_{q,l} \left(\frac{\hat{m}_f}{\exp[\hat{\beta}(x_{\max} - x_f)]} \right) = \mathcal{D}_f.$$

3.2 Spline Knots Selection

The number of knots and knot locations are a key component to using B-splines to model the degradation path. In addition, it is also necessary to determine the maximum degree of the B-splines. For knot selection, we first fix the degree of the B-splines and then find the optimum knot locations. Optimality is determined by a variation of the Akaike information criterion:

$$\text{AIC} = -2 \log \left\{ \frac{1}{\sqrt{2\pi} |\hat{\Sigma}|^{1/2}} \exp \left[-\frac{(\mathbf{y} - \mathbf{X}_{\hat{\beta}} \hat{\boldsymbol{\gamma}}) \hat{\Sigma}^{-1} (\mathbf{y} - \mathbf{X}_{\hat{\beta}} \hat{\boldsymbol{\gamma}})}{2} \right] \right\} + 2 \times \text{edf}, \quad (10)$$

where edf is the effective degrees of freedom in $\boldsymbol{\gamma}$ plus three for the parameters $(\beta, \sigma, \rho)'$. Wang, Meyer, and Opsomer (2013) and Meyer (2012) discussed constrained spline regression for both independent and correlated error cases. In particular, they showed how to calculate the effective degrees of freedom for a constrained fit through the use of a cone projection, which is the trace of the projection matrix. Because we have $p - 1$ linear constraints, the effective degrees of freedom in $\boldsymbol{\gamma}$ has a value from 1 to p , where p corresponds to a unconstrained fit. Letting q denote the degree of the B-spline functions, the procedure for knot selection is as follows:

1. Determine the optimum number of interior knots $N_{\text{opt},q}$ which minimizes the AIC. The default knot locations are equally-spaced sample quantiles. That is, if number of interior knots is N , the default knot locations are $b/N, b = 1, \dots, N - 1$.
2. Delete each of the internal knots in sequence. The knot whose deletion leads to the greatest reduction in AIC is removed. Repeat until no more existing knots can be removed.

The whole procedure is to be repeated for different B-spline degrees until the optimal knot sequence is determined. This knot selection procedure is similar to the procedure in

He and Shi (1998). The sample size for an ADDT is typically small and so a low degree of spline ($q \leq 4$) and a small number of interior knots ($1 \leq N \leq 5$) are usually sufficient to provide a good fit to the data.

3.3 Statistical Inference

Inference based on the semi-parametric model in (7) can rely on either asymptotic theory or a bootstrap procedure. Because the bootstrap method is straightforward and easy to implement, we use a nonparametric bootstrap to calculate confidence intervals (CI) for the parameters and pointwise CI for the degradation path. The error term in model (7) can be written as

$$\varepsilon_{ijk} = u_{ij} + e_{ijk},$$

where $u_{ij} \sim N(0, \sigma_u^2)$, $e_{ijk} \sim N(0, \sigma_e^2)$, $\text{Corr}(u_{ij}, e_{ijk}) = 0$, $\sigma_u^2 = \rho\sigma^2$, and $\sigma_e^2 = (1 - \rho)\sigma^2$. That is, the error term in model (7) can be written as the sum of a random effect term u_{ij} and an independent error term e_{ijk} . To obtain the CI, one could resample from the estimated random effect term \hat{u}_{ij} and the estimated independent error term \hat{e}_{ijk} separately. However, Carpenter, Goldstein, and Rasbash (2003) showed that directly resampling from \hat{u}_{ij} and \hat{e}_{ijk} will cause bias. Therefore, we adjust \hat{u}_{ij} and \hat{e}_{ijk} prior to bootstrapping. That is,

$$\hat{u}_{ij}^c = \left[\sum_{ij} \hat{u}_{ij}^2 / (nJ_n) \right]^{-1/2} \hat{\sigma}_u \hat{u}_{ij}, \quad \text{and} \quad \hat{e}_{ijk}^c = \left[\sum_k \hat{e}_{ijk}^2 / (n_{ij}) \right]^{-1/2} \hat{\sigma}_e \hat{e}_{ijk}.$$

The specific steps of nonparametric bootstrap are described as follows:

For $m = 1, \dots, B$,

1. Sample $u_{ij}^{(m)c}$ with replacement from \hat{u}_{ij}^c and sample $e_{ijk}^{(m)c}$ with replacement from \hat{e}_{ijk}^c .
2. Compute $y_{ijk}^{(m)} = x'_{ij} \hat{\gamma} + u_{ij}^{(m)c} + e_{ijk}^{(m)c}$.
3. Fit the semi-parametric model to the bootstrapped sample $y_{ijk}^{(m)}$.

The CI with confidence level $1 - \alpha$ for a parameter of interest, θ , is calculated by taking the lower and upper $\alpha/2$ quantiles of the bootstrap estimates. For a sequence of bootstrap estimates $\hat{\theta}^{(1)}, \dots, \hat{\theta}^{(B)}$, a bias-corrected CI, proposed by Efron and Tibshirani (1993), can be computed by taking the $B\Phi(2z_q + z_{\alpha/2})$ and $B\Phi(2z_q + z_{1-\alpha/2})$ ordered values, where q denotes the proportion of bootstrap values less than $\hat{\theta}$, $\Phi(\cdot)$ is the cumulative distribution function and $z_{(\cdot)}$ is the quantile function of the standard normal distribution.

4 Simulation Study

The objective of the simulation study is to investigate the performance of the proposed parameter estimation and inference procedures. We will examine the bias, standard deviation (SD), and mean square error (MSE) of the parameter estimators and the estimated baseline degradation function. We also will investigate the coverage probability (CP) of the bootstrap-based CI procedure in Section 3.3. An additional simulation study will be conducted to investigate the performance of our semi-parametric model under model misspecification.

4.1 Performance of Parameter Estimators

Simulation Settings

We consider two different sets of $n = \{3, 6\}$ temperature levels and three different sets of $J_n = \{5, 10, 15\}$ measuring times. The specific settings are summarized in Table 1. Ten samples are tested at each combination of temperature level and measuring times. The data are simulated from the following model:

$$y_{ijk} = \sum_{l=1}^p r_l B_{q,l}[\eta_i(t_{ij}; \beta)] + \varepsilon_{ijk}, \quad (11)$$

where the degree of the B-splines is $q = 2$, and number of interior knots is $N = 3$. The knot locations are the sample quantiles. Figure 1 gives the spline basis functions and the baseline degradation function for scenario $n = 3$, $J_n = 5$. The true parameters in the model are $\beta = 0.83$, $\gamma = (1, 0.9, 0.8, 0.7, 0.6, 0.6)'$, and $(\sigma, \rho)' = (0.019, 0.2)'$.

For each scenario, 500 datasets are generated and the bias, SD, and MSE of the parameter estimators and baseline degradation curves are calculated. The quantile and bias-corrected CI are computed based on $B = 1,000$ bootstrap samples and the CP is also computed.

Simulation Results

Figure 2 shows the bias and MSE of parameter estimators. Figure 3 shows the pointwise MSE curves of baseline degradation curves. We found out that MSE of point estimators and baseline degradation curves decrease as either number of temperature levels or time points increases. Even when the number of temperature levels and time points are both small, biases of β and σ are small, while bias of ρ is large. However, when either number of temperature levels or time points is large, the estimates of β , σ and ρ are all close to the true values.

Table 1: Selected temperature levels and time points for the simulation studies.

Settings	Number of Temp. Levels (n)	Temperature Levels ($^{\circ}\text{C}$)
Temperature setting 1	3	50, 65, 80
Temperature setting 2	6	30, 40, 50, 60, 70, 80
	Number of Time Points (J_n)	Measuring Times (Hours)
Time point setting 1	5	8, 25, 75, 130, 170
Time point setting 2	10	5, 10, 30, 50, 70, 90, 110, 130, 150, 170
Time point setting 3	15	10, 30, 40, 50, 60, 70, 80, 90, 100, 110, 120, 130, 140, 150, 170

Figures 4 and 5 present the CP for quantile-based CI and bias-corrected CI of the parameter estimators and baseline degradation curves. The performance of bias-corrected CI seems to be similar for β , and better for σ , ρ and baseline degradation curve compared to quantile-based CI. For the parameter estimators, the CP of bias-corrected CI of β is good when n or J_n is small. However, the CP of bias-corrected CI of $(\sigma, \rho)'$ are overall slightly less than the desired confidence level. For the baseline degradation function, the CP of pointwise bias-corrected CI are poor when $n = 3$ and $J_n = 5$. The performance of pointwise bias-corrected CI improve as n and J_n increases. Overall, the results show that the performance of the estimation and inference procedures are good.

4.2 Performance under Model Misspecification

Simulation Settings

In this simulation study, the data are simulated according to a parametric model, but the semi-parametric model is fit to the data. The temperature levels are set at 50°C , 65°C , 80°C and the measuring times are set at 192, 600, 1800, 3120, and 4320 hours. There are 10 measurements at time 0 and 5 measurements at all other measuring times. The data are simulated from the model

$$y_{ijk} = \beta_0 + \beta_1 \exp(\beta_2 x_i) \tau_j + \varepsilon_{ijk}, \quad (12)$$

where $\tau_j = \text{Hour}_j$, $x_i = -11605/(\text{Temp}_i + 273.15)$. The true parameters are $\boldsymbol{\beta} = (\beta_0, \beta_1, \beta_2)' = (1, -3.5, 0.3)'$, and $(\sigma, \rho)' = (0.02, 0)'$. It is rare for the true model to be known exactly, so we also consider the case when a different parametric model from the true one is fit to the data. The incorrect parametric model, adapted from Vaca-Trigo and Meeker (2009), is given

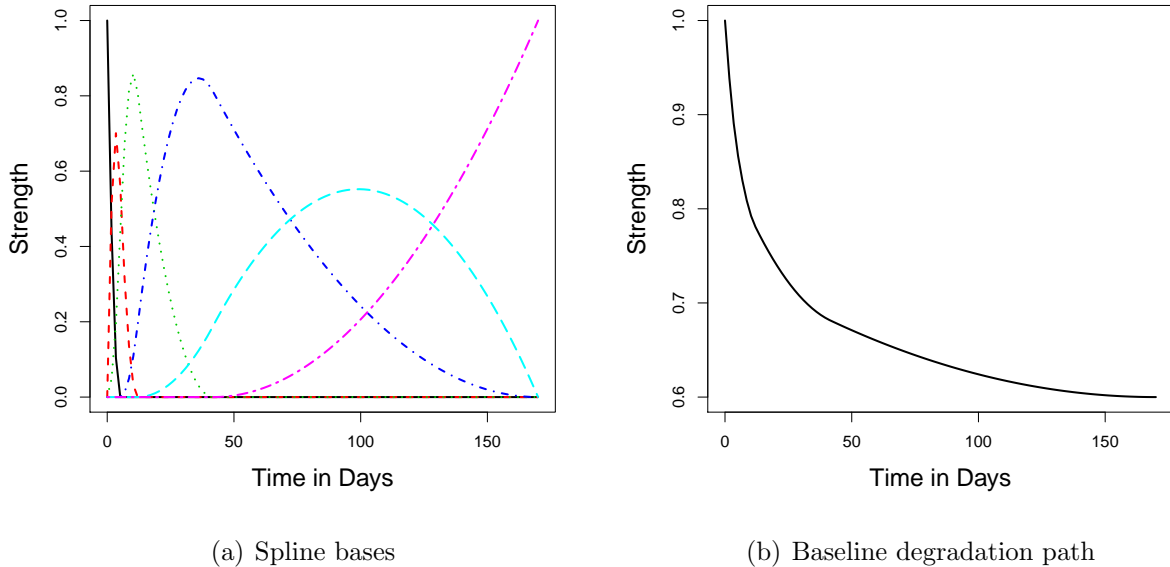


Figure 1: Spline bases and baseline degradation path used in simulation study.

by

$$y_{ijk} = \frac{\alpha}{1 + \left[\frac{t_{ij}}{\exp(\beta_0 + \beta_1 x_i)} \right]^\gamma} + \varepsilon_{ijk}, \quad (13)$$

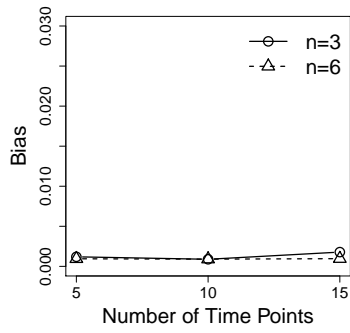
with parameters $(\alpha, \beta_0, \beta_1, \gamma)'$ in the mean structure. We fit the true model (12), the incorrect parametric model (13), and our semi-parametric model (3) to the simulated data. Figure 6 shows one case of the simulated data and the fitted degradation paths.

Simulation Results

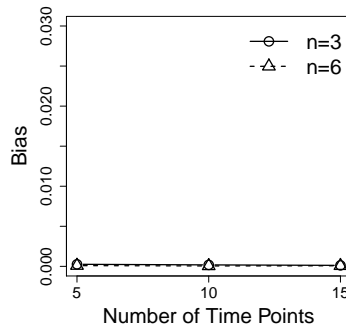
To assess the fit of our semi-parametric model, we compare the fitted degradation path to the true degradation path using the integrated mean square error (IMSE) of the baseline degradation function, which is defined as

$$\begin{aligned} \text{IMSE} &= \int_0^{t_m} \mathbf{E} \{ [\hat{g}(t; \gamma) - g(t; \gamma)]^2 \} dt \\ &= \int_0^{t_m} \{ \mathbf{E} [\hat{g}(t; \gamma)] - g(t; \gamma) \}^2 dt + \int_0^{t_m} \text{Var} [\hat{g}(t; \gamma)] dt = \text{IBias}^2 + \text{IVar}, \end{aligned}$$

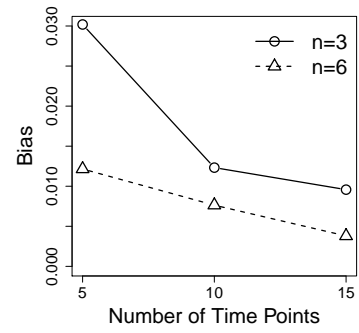
where t_m is the maximum time under the maximum level of the accelerating variable. As there is no closed-form expressions for IMSE, IBias and IVar, we report the empirical results. Table 2 presents these results, which indicate that the performance of our semi-parametric



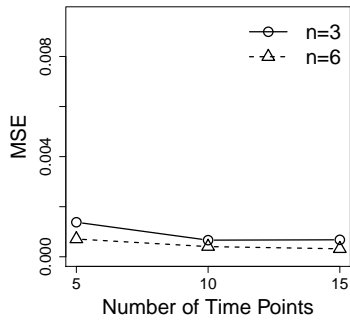
(a) β



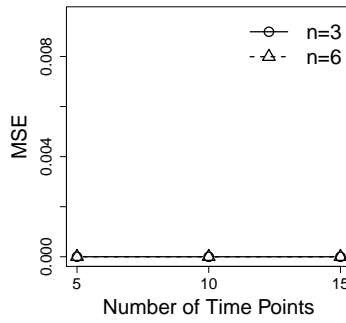
(b) σ



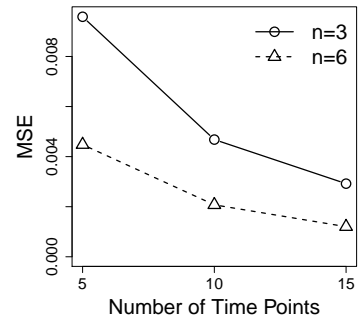
(c) ρ



(d) β



(e) σ



(f) ρ

Figure 2: Empirical bias and MSE of parameter estimators for $(\beta, \sigma, \rho)'$.

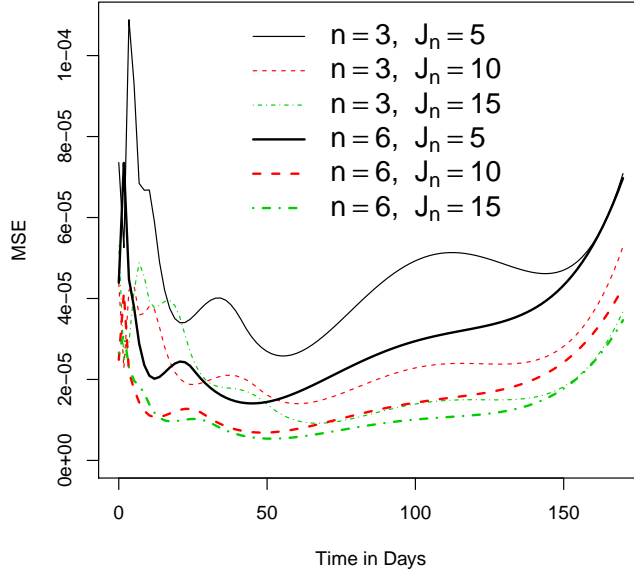


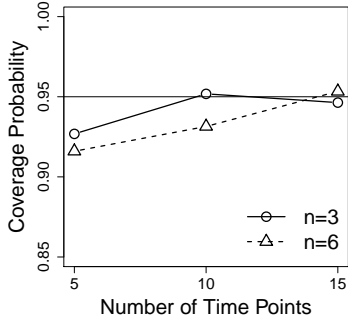
Figure 3: Empirical pointwise MSE for the estimator of the baseline degradation path.

Table 2: Empirical IBias, root IVar (RIVar), and root IMSE (RIMSE) for the true model (12), incorrect model (13), and the semi-parametric model.

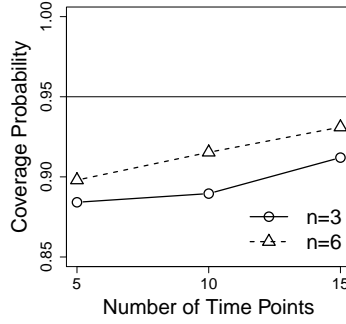
Models	IBias	RIVar	RIMSE
True Model	0.0003	0.0043	0.0043
Incorrect Model	0.0267	0.0060	0.0274
Semi-parametric Model	0.0003	0.0091	0.0091

model is good. The largest contribution to the root IMSE comes from the variance component. Thus, it is not surprising that the incorrect parametric model (13) performs the worst in capturing the true degradation path.

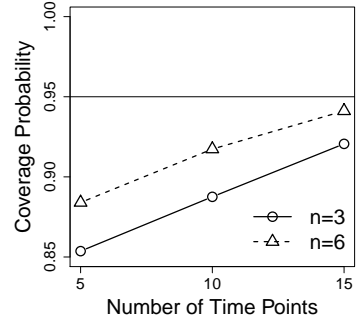
For each simulated dataset, the MTTF at 30°C is calculated based on the true parametric model (12), incorrect parametric model (13) and the semi-parametric model. The mean, bias, standard derivation and root MSE of the MTTF for each of the different models based on 600 datasets are summarized in Table 3. The results indicate that the estimate of MTTF from our semi-parametric model is close to the true values, but with larger variance. The estimated MTTF from the incorrect parametric model (13) has the largest bias. The results indicate our semi-parametric model performs quite well.



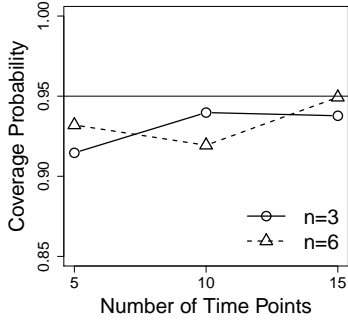
(a) β , Quantile-based CI



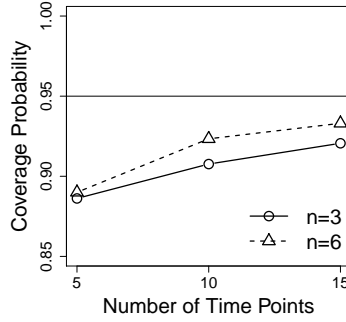
(b) σ , Quantile-based CI



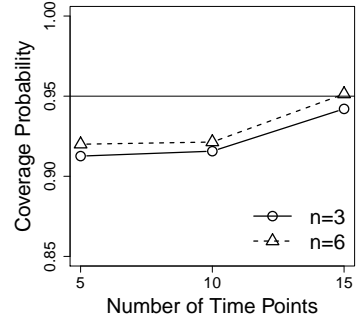
(c) ρ , Quantile-based CI



(d) β , Bias-corrected CI



(e) σ , Bias-corrected CI

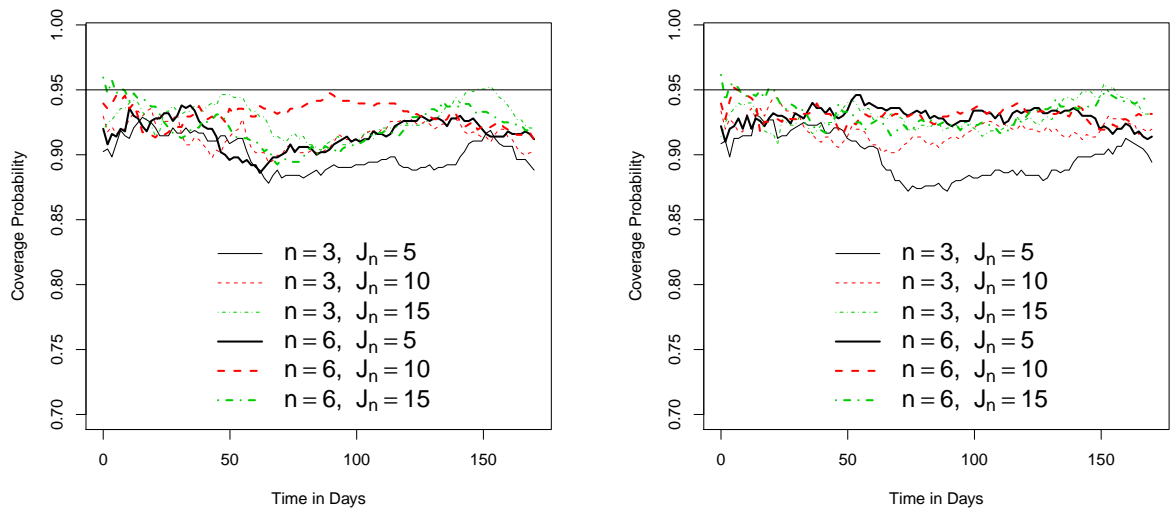


(f) ρ , Bias-corrected CI

Figure 4: CP of the CI procedures for parameters $(\beta, \sigma, \rho)'$, using quantile-based and bias-corrected methods, respectively.

Table 3: Empirical mean, bias, SD, and root MSE (RMSE) of the MTTF estimators based on the true model (12), incorrect model (13), and the semi-parametric model.

Models	Mean	Bias	SD	RMSE
True Model	82.60	0.01	2.99	2.99
Incorrect Model	85.82	3.20	3.75	4.93
Semi-parametric Model	82.77	0.16	4.22	4.22



(a) Quantile-based CI

(b) Bias-corrected CI

Figure 5: Pointwise CP of the CI procedure for baseline degradation path, using quantile-based and bias-corrected methods, respectively.

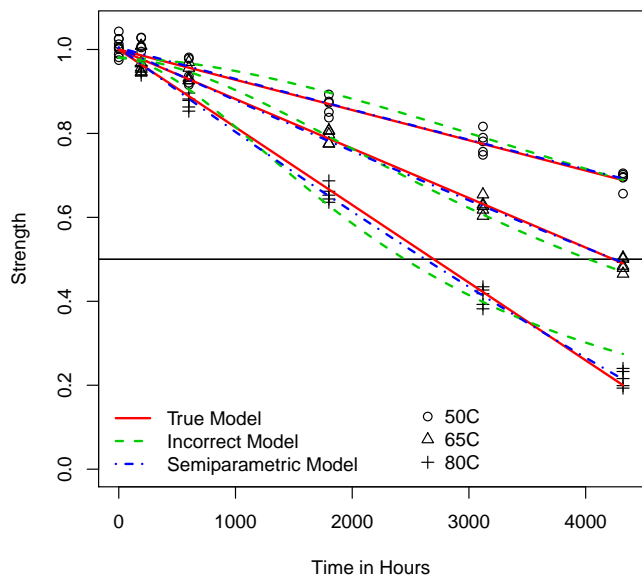


Figure 6: Plot of simulated data and fitted degradation paths based on the true and incorrect parametric models, and semi-parametric model.

5 Applications

To help motivate the use of our semi-parametric model, we selected three published datasets from well-known examples of ADDT. The data for each example are summarized below.

5.1 ADDT Datasets and Parametric Models

Adhesive Bond B Data

Escobar et al. (2003) discussed an experiment that measured the strength of an adhesive bond (Adhesive Bond B) over time. Eight units were measured at the beginning of the experiment under normal temperature to serve as the baseline strength. The remaining measurements were taken at selected weeks (2, 4, 6, 12, and 16) for three accelerated temperature levels (50°C, 60°C, and 70°C). A scatter plot of Adhesive Bond B dataset is presented in Figure 7(a). The degradation model used by Escobar et al. (2003) is

$$y_{ijk} = \beta_0 + \beta_1 \exp(\beta_2 x_i) \tau_j + \varepsilon_{ijk}, \quad (14)$$

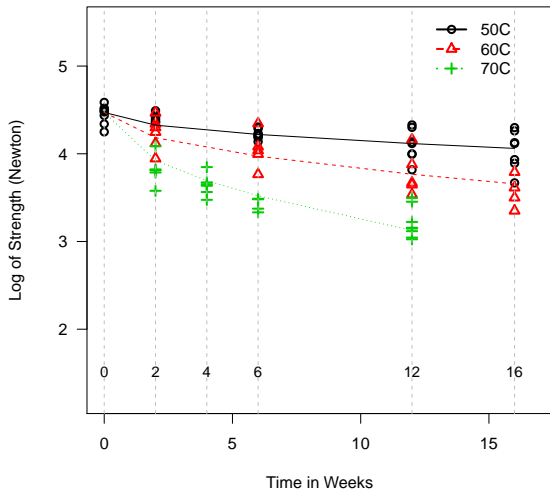
where y_{ijk} is the strength of Adhesive Bond B in log Newtons, $\tau_j = \sqrt{\text{Week}_j}$, $x_i = -11605/(\text{Temp}_i + 273.15)$ is the Arrhenius-transformed temperature, and $\varepsilon_{ijk} \sim N(0, \sigma^2)$. The estimates are $\hat{\beta}_0 = 4.4713$, $\hat{\beta}_1 = -8.6384 \times 10^8$, $\hat{\beta}_2 = 0.6364$ and $\hat{\sigma} = 0.1609$.

Seal Strength Data

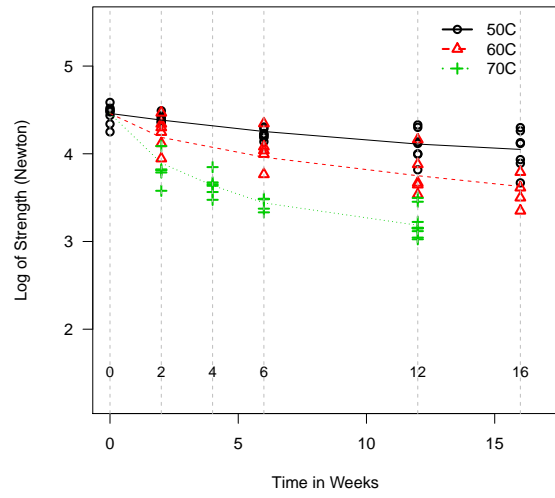
Seal strength data were considered by Li and Doganaksoy (2014). At the start of the experiment, a batch of 10 seals were measured at the use temperature level of 100°C. A batch of 10 seal samples were then tested at selected weeks (5, 10, 15, 20, and 25) for four temperature levels (200°C, 250°C, 300°C, and 350°C). A scatter plot of seal strength data is shown in Figure 8(a). Though one would expect the seal strength to decrease under higher temperature, some batches of seal samples yielded higher strengths in later weeks compared with the initial measurements. This suggests a large batch-to-batch variability which must be incorporated into the model. Thus, Li and Doganaksoy (2014) considered the following nonlinear mixed model:

$$y_{ijk} = \beta_0 - \beta_1 \exp(\beta_2 x_i) \tau_j + \delta_{ij} + \varepsilon_{ijk}, \quad (15)$$

where y_{ijk} is the \log_{10} strength of seal sample, $\tau_j = \text{Week}_j$, and $x_i = -11605/(\text{Temp}_i + 273.15)$. The random variable $\delta_{ij} \sim N(0, \sigma_\delta^2)$ represents batch variability, $\varepsilon_{ijk} \sim N(0, \sigma^2)$, and δ_{ij} and ε_{ijk} are independent. The estimates are $\hat{\beta}_0 = 1.4856$, $\hat{\beta}_1 = 47.2166$, $\hat{\beta}_2 = 0.3420$, $\hat{\sigma} = 0.1603$, and $\hat{\sigma}_\delta = 0.0793$.

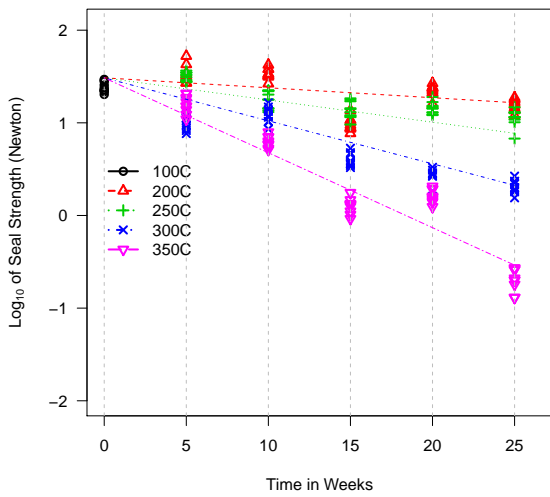


(a) Parametric model

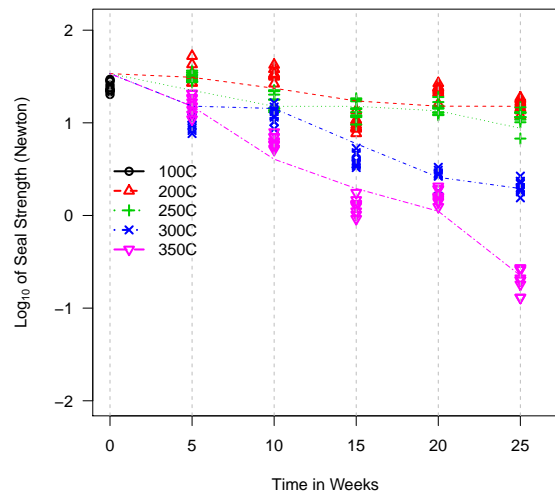


(b) Semi-parametric model

Figure 7: Fitted degradation paths of the Adhesive Bond B data.



(a) Parametric model



(b) Semi-parametric model

Figure 8: Fitted degradation paths of the Seal Strength data.

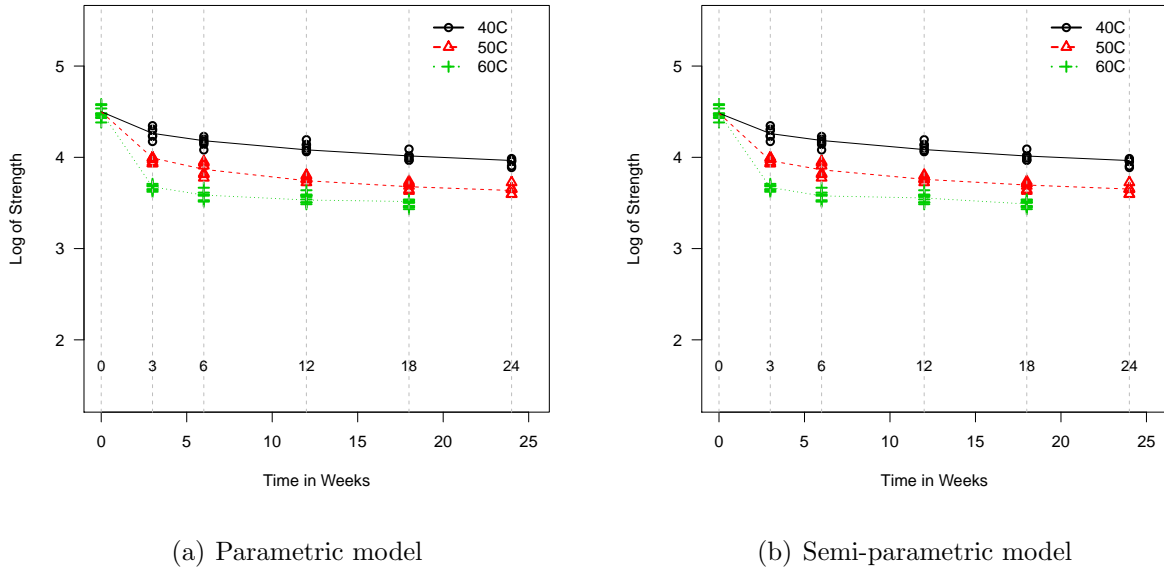


Figure 9: Fitted degradation paths of the Adhesive Formulation K data.

Adhesive Formulation K Data

A new adhesive (Formulation K) was developed and tested at 40°C, 50°C, and 60°C. The strength of 10 units were measured at the beginning of the experiment and a specified number of samples were tested at 3, 6, 12, 18, and 24 weeks. Figure 9(a) is a scatter plot of the data. The nonlinear degradation model is

$$y_{ijk} = \log(90) + \beta_0(1 - \exp\{-\beta_1 \exp[\beta_2(x_i - x_2)] \tau_j\}) + \varepsilon_{ijk}, \quad (16)$$

where y_{ijk} is the strength of Adhesive Formulation K in log Newtons, $\tau_j = \sqrt{\text{Week}_j}$, $x_i = -11605/(\text{Temp}_i + 273.15)$, $x_2 = -11605/(50 + 273.15)$, and $\varepsilon_{ijk} \sim N(0, \sigma^2)$. The estimates are $\hat{\beta}_0 = -0.9978$, $\hat{\beta}_1 = 0.4091$, $\hat{\beta}_2 = 0.8371$, and $\hat{\sigma} = 0.0501$.

5.2 Comparisons of Parametric and Semi-parametric Models

In order to assess the fit of the semi-parametric model, we applied it to each of the datasets and compared it with the corresponding parametric model chosen by the respective applications. We applied the knot selection technique in Section 3.2 for each application. We also tested the significance of $\rho = 0$ which informs the selection of the appropriate model. The parameter estimates and CI, as well as the MTTF at the normal use condition are presented in Tables 4 and 5. The AIC defined in Section 3.2 can also be used to compare

Table 4: Parameter estimates and corresponding CI for the semi-parametric models for the three applications.

Applications	Parameter	Estimate	Quantile-based CI	
			95% lower	95% upper
Adhesive Bond B	β	1.3422	1.1071	1.6165
	σ	0.1537	0.1265	0.1787
Seal Strength	β	0.3235	0.2451	0.5194
	σ	0.1610	0.1192	0.1904
	ρ	0.7573	0.5465	0.8307
Adhesive Formulation K	β	1.8221	1.6575	2.3658
	σ	0.0484	0.0419	0.0544

Table 5: Estimated MTTF at normal use condition based on parametric and semi-parametric models for the three applications (time in weeks).

Applications	Failure Threshold	Normal Use Conditions	Parametric Models	Semi-parametric Models
Adhesive Bond B	70%	30°C	270	306
Seal Strength	70%	100°C	222	127
Adhesive Formulation K	70%	30°C	68	92

the parametric and semi-parametric models. In the calculation of AIC, the log-likelihood is the marginal log-likelihood for the parametric models.

Table 6 contains the log-likelihood values, edf , and AIC for each model and dataset. For all three datasets, the semi-parametric models possessed a lower AIC as compared to the parametric models. The fitted degradation paths for the parametric and semi-parametric models are presented in Figures 7, 8, and 9. All three figures show that the semi-parametric models provide a good fit to the data. We can see that the proposed model is flexible in fitting ADDT data from different applications.

Table 6: Log likelihood and AIC values of parametric and semi-parametric models for the ADDT data from the three applications.

Applications	Parametric Models			Semi-parametric Models		
	Loglik	df	AIC	Loglik	edf	AIC
Adhesive Bond B	34.9665	4	-61.9330	38.7264	5	-67.4418
Seal Strength	194.9907	5	-379.9814	199.7454	6	-387.4909
Adhesive Formulation K	158.9508	4	-309.9016	163.9898	8	-311.9797

6 Conclusions and Areas for Future Work

In this paper, we describe a new semi-parametric degradation model for ADDT data based on monotone B-splines. We develop estimation and inference procedures for the proposed model as well as methods for selecting knot locations for the B-splines. Our simulation results indicate that the proposed estimation procedures for our semi-parametric model perform very well. Compared to parametric models, our semi-parametric approach is more flexible and can be applied to a wide range of applications and may be best suited as a generic method for ADDT data analysis for industrial standards. In addition, the semi-parametric model is more robust to model misspecification than a parametric model approach.

One key application of our semi-parametric model could be for test planning. A test plan based on this model would be general enough for application to a variety of materials and also allow for testing of different models. Our model can be served as a starting ground from which to test models against the data gathered rather than having to assume a given model prior to data collection. This would certainly serve as an interesting topic for future research.

The models considered here were solely scale-acceleration models. However, for certain types of products, a model with both scale and shape acceleration may describe the degradation path more appropriately. For example, Tsai et al. (2013) considered a parametric model with both scale and the shape acceleration in test planning. Estimation and inference procedures for the semi-parametric model would certainly be more complex with the introduction of a shape acceleration parameter. It would be of great interest to pursue this in future research.

References

- Bollaerts, K., P. H. Eilers, and I. Mechelen (2006). Simple and multiple p-splines regression with shape constraints. *British Journal of Mathematical and Statistical Psychology* 59(2), 451–469.
- Carpenter, J. R., H. Goldstein, and J. Rasbash (2003). A novel bootstrap procedure for assessing the relationship between class size and achievement. *Applied Statistics* 52, 431–443.
- De Boor, C. (2001). *A practical guide to splines*. New York: Springer-Verlag.
- Efron, B. and R. Tibshirani (1993). *An Introduction to the Bootstrap*. FL: Boca Raton: Chapman and Hall/CRC.

- Eilers, P. H. and B. D. Marx (1996). Flexible smoothing with b-splines and penalties. *Statistical science*, 89–102.
- Escobar, L. A., W. Q. Meeker, D. L. Kugler, and L. L. Kramer (2003). Accelerated destructive degradation tests: Data, models, and analysis. *Mathematical and Statistical Methods in Reliability*, 319–338.
- Fengler, M. R. and L.-Y. Hin (2014). A simple and general approach to fitting the discount curve under no-arbitrage constraints. *Available at SSRN*: <http://ssrn.com/abstract=2478719>.
- Fritsch, F. N. and R. E. Carlson (1980). Monotone piecewise cubic interpolation. *SIAM Journal on Numerical Analysis* 17(2), 238–246.
- Gorjian, N., L. Ma, M. Mittinty, P. Yarlagadda, and Y. Sun (2010). A review on degradation models in reliability analysis. In *Engineering Asset Lifecycle Management*, pp. 369–384. Springer.
- He, X. and P. Shi (1998). Monotone b-spline smoothing. *Journal of the American statistical Association* 93(442), 643–650.
- Hofner, B., T. Kneib, and T. Hothorn (2014). A unified framework of constrained regression. *Statistics and Computing*, 1–14.
- Hofner, B., J. Müller, and T. Hothorn (2011). Monotonicity-constrained species distribution models. *Ecology* 92(10), 1895–1901.
- Hong, Y., Y. Duan, W. Q. Meeker, D. L. Stanley, and X. Gu (2015). Statistical methods for degradation data with dynamic covariates information and an application to outdoor weathering data. *Technometrics* 57, 180–193.
- Kanungo, T., D. M. Gay, and R. M. Haralick (1995). Constrained monotone regression of roc curves and histograms using splines and polynomials. In *Image Processing, 1995. Proceedings., International Conference on*, Volume 2, pp. 292–295. IEEE.
- Leitenstorfer, F. and G. Tutz (2007). Generalized monotonic regression based on b-splines with an application to air pollution data. *Biostatistics* 8(3), 654–673.
- Li, M. and N. Doganaksoy (2014). Batch variability in accelerated-degradation testing. *Journal of Quality Technology* 46, 171–180.
- Lu, C. J. and W. Q. Meeker (1993). Using degradation measures to estimate a time-to-failure distribution. *Technometrics* 34, 161–174.
- Meeker, W. Q., L. A. Escobar, and C. J. Lu (1998). Accelerated degradation tests: modeling and analysis. *Technometrics* 40(2), 89–99.

- Meeker, W. Q., Y. Hong, and L. A. Escobar (2011). Degradation models and data analyses. In *Encyclopedia of Statistical Sciences*. Wiley.
- Meyer, M. (2012). Constrained penalized splines. *Canadian Journal of Statistics* 40, 190–206.
- Meyer, M. C. (2008). Inference using shape-restricted regression splines. *The Annals of Applied Statistics* 2, 1013–1033.
- Nelson, W. B. (1990). *Accelerated testing: statistical models, test plans, and data analysis*. John Wiley & Sons.
- Ramsay, J. O. (1988). Monotone regression splines in action. *Statistical science* 3, 425–441.
- Tsai, C.-C., S.-T. Tseng, N. Balakrishnan, and C.-T. Lin (2013). Optimal design for accelerated destructive degradation tests. *Quality Technology and Quantitative Management* 10, 263–276.
- UL746B (2013). *Polymeric Materials - Long Term Property Evaluations, UL 746B*. Underwriters Laboratories, Incorporated.
- Vaca-Trigo, I. and W. Q. Meeker (2009). A statistical model for linking field and laboratory exposure results for a model coating. In J. Martin, R. A. Ryntz, J. Chin, and R. A. Dickie (Eds.), *Service Life Prediction of Polymeric Materials*, Chapter 2. NY: New York: Springer.
- Wang, H., M. C. Meyer, and J. D. Opsomer (2013). Constrained spline regression in the presence of AR(p) errors. *Journal of Nonparametric Statistics* 25, 809–827.
- Xu, Z., Y. Hong, and R. Jin (2015). Nonlinear general path models for degradation data with dynamic covariates. *Applied Stochastic Models in Business and Industry*, in press, doi: 10.1002/asmb.2129.
- Ye, Z. and M. Xie (2015). Stochastic modelling and analysis of degradation for highly reliable products. *Applied Stochastic Models in Business and Industry* 31, 16–32.
- Ye, Z.-S., M. Xie, L.-C. Tang, and N. Chen (2014). Semiparametric estimation of Gamma processes for deteriorating products. *Technometrics* 56, 504–513.